Published in final edited form as:
J Perinat Med. 2006 ; 34(1): 39–55.

Four-Dimensional Ultrasonography of the Fetal Heart using a Novel Tomographic Ultrasound Imaging Display

Luís F. Gonçalves[1,2], **Jimmy Espinoza**[1,2], **Roberto Romero**[1], **Juan Pedro Kusanovic**[1,2], **Betsy Swope**[1,2], **Jyh Kae Nien**[1], **Offer Erez**[1,2], **Eleazar Soto**[1,2], and **Marjorie C. Treadwell**[2]

1*Perinatology Research Branch, National Institute of Child Health and Human Development, NIH/DHHS, Bethesda, Maryland and Detroit, Michigan USA*

2*Department of Obstetrics and Gynecology, Wayne State University/Hutzel Women's Hospital, Detroit, Michigan USA*

Abstract

Objective—The objective of this study was to investigate the feasibility of examining the fetal heart with Tomographic Ultrasound Imaging (TUI) using four-dimensional (4D) volume datasets acquired with spatiotemporal image correlation (STIC).

Material and Methods—One hundred and ninety-five fetuses underwent 4D ultrasonography (US) of the fetal heart with STIC. Volume datasets were acquired with B-mode (n=195) and color Doppler imaging (CDI) (n=168), and were reviewed offline using TUI, a new display modality that automatically slices 3D/4D volume datasets, providing simultaneous visualization of up to eight parallel planes in a single screen. Visualization rates for standard transverse planes used to examine the fetal heart were calculated and compared for volumes acquired with B-mode or CDI. Diagnoses by TUI were compared to postnatal diagnoses.

Results—1) The four- and five-chamber and the three-vessel and trachea views were visualized in 97.4% (190/195), 88.2% (172/195), and 79.5% (142/195), respectively, of the volume datasets acquired with B-mode; 2) these views were visualized in 98.2% (165/168), 97.0% (163/168), and 83.6% (145/168), respectively, of the volume datasets acquired with CDI; 3) CDI contributed additional diagnostic information to 12.5% (21/168), 14.2% (24/168) and 10.1% (17/168) of the four- and five-chamber and the three-vessel and trachea views; 4) cardiac anomalies other than isolated ventricular septal defects were identified by TUI in 16 of 195 fetuses (8.2%) and, among these, CDI provided additional diagnostic information in 5 (31.3%); 5) the sensitivity, specificity, positive- and negative-predictive values of TUI to diagnose congenital heart disease in cases where both B-mode and CDI volume datasets were acquired prenatally were 92.9%, 98.8%, 92.9% and 98.8%, respectively.

Conclusion—Standard transverse planes commonly used to examine the fetal heart can be automatically displayed with TUI in the majority of fetuses undergoing 4D US with STIC. Due to the retrospective nature of this study, the results should be interpreted with caution and independently confirmed before this methodology is introduced into clinical practice.

Keywords

Fetal echocardiography; 3D, 4D, three-dimensional, four-dimensional; STIC; spatiotemporal; congenital heart disease; spatiotemporal; prenatal diagnosis; 3D, 4D

Corresponding author: Roberto Romero, MD, Perinatology Research Branch, NICHD, NIH, DHHS, Wayne State University/Hutzel Women's Hospital, 3990 John R, Box 4, Detroit, MI 48201, Tel: 313-993-2700, Fax: 313-993-2694, e-mail:warfiela@mail.nih.gov.

Introduction

Severe congenital heart disease is present in approximately 6 of every 1,000 live births and is the leading cause of death among infants with congenital anomalies.[38,39] When trivial defects with minor or no clinical significance such as small muscular ventricular septal defects (VSDs) present at birth are included in the analysis, the incidence may be as high as 75/1,000 live births.[38,57,59] Prenatal diagnosis of congenital heart disease [e.g. transposition of the great arteries, hypoplastic left heart syndrome, and coarctation of the aorta] is associated with a decrease in neonatal morbidity and mortality.[9,26,47,70] However, prenatal diagnosis of congenital heart disease by two-dimensional (2D) ultrasound relies heavily on operator skills, and the detection rates in population based studies range from 6 to 35%.[11,15,25,27,34,40, 42,58,66,67,69] Since the dependency on operator skills is considered by many as the limiting factor in improving the detection rates for congenital heart disease,[3,68] several investigators have explored the use of three-dimensional (3D) and four-dimensional (4D) ultrasound for the examination of the fetal heart.[1,2,4,5,7,8,10,12,13,16–24,28–30,32,33,35–37,41,45,46,48–56,60–65,71,72,74,76]

In 2002, Yagel et al.[73] proposed a method to streamline the examination of the fetal heart, based on the evaluation of five transverse planes: 1) the transverse view of the upper abdomen; 2) the four-chamber view; 3) the five-chamber view; 4) the three-vessel view; and 5) the three-vessel view and trachea view (Figure 1).[73] This method has the potential to simplify the examination of the fetal heart by minimizing the need to obtain several short and long axis views of the heart. These views may be difficult to obtain due to an unfavorable fetal position or lack of operator experience.[73] Subsequently, Chaoui and McEwing[14] proposed that the evaluation of only three planes of section with color Doppler (the four- and five-chamber and three-vessel views) would be sufficient to identify most cases of congenital heart disease.

Spatiotemporal image correlation (STIC) is a commercially available technology for 4D ultrasonographic examination of the fetal heart. Volume datasets are acquired over a period of 7.5 to 15 seconds and can be analyzed either in the presence of the patient or offline in a computer workstation. Several techniques have been proposed to evaluate the fetal heart by 4D ultrasound with STIC, including multiplanar display to visualize the planes of section required to conduct a basic and extended examination of the fetal heart, as well as rendering techniques to display 4D images of specific cardiac structures such as the atrioventricular valves, outflow tracts, aortic arch, ductal arch, and venous return to the heart.[8,13,21–24, 28–30,32,33,71,72,74]

Recently, ultrasound manufacturers have developed software that automatically slices volume datasets acquired by 3D and 4D ultrasonography (Multislice View™, Accuvix, Medison, Seoul, Korea; Tomographic Ultrasound Imaging, Voluson 730, General Electric Medical Systems, Kretztechnik, Zipf, Austria). Such software produces a series of tomographic images, akin to display methods used by diagnostic imaging professionals to review computerized tomography and magnetic resonance imaging studies. This novel display modality has been recently described for prenatal visualization of anatomic fetal structures and to diagnose congenital anomalies.[44] In the current study, we investigate the feasibility of examining the fetal heart with Tomographic Ultrasound Imaging (TUI) in 4D volume datasets acquired with STIC. Specifically, we sought to determine whether the five planes of section proposed by Yagel et al.[73] and the three planes of section proposed by Chaoui and McEwing[14] could be automatically obtained using this new modality.

Material and Methods

Four-dimensional volume datasets of the fetal heart were acquired with transverse sweeps through the fetal chest in 195 patients examined at our ultrasound unit between December 1st 2003 and December 31st 2004. Examinations were performed with STIC (Voluson 730 Expert, release BTO4, General Electric Medical Systems, Kretztechnik, Zipf, Austria) using hybrid mechanical and curved array transducers (RAB 4-8P, RAB 4-8L, RAB 2-5P, RAB 2-5L). Patients were examined between 14 and 41 weeks of gestation (median 24 1/7 weeks; interquartile range: 15 3/7 to 32 6/7 weeks). All patients were enrolled in research protocols approved by the Institutional Review Board of the National Institute of Child Health and Human Development (NICHD/NIH/DHHS) and by the Human Investigation Committee of Wayne State University (Detroit, Michigan); all signed a written informed consent prior to participation in the study.

After removal of patient identifiers, examinations were retrospectively reviewed offline on a personal computer using the 4D View software version 5.0 (4D VIEW 5.0, General Electric Medical Systems, Kretztechnik, Zipf, Austria). Even though some of the patients were examined more than once during pregnancy and multiple volume datasets were acquired in the course of each scanning session, a maximum of two volume datasets per patient (one acquired with B-mode imaging and one with color Doppler) were included in the study. Preference was given to volume datasets acquired between 16 and 24 weeks of gestation, when available, and the volume dataset considered by the investigator to be of highest quality was selected. Volume datasets with the following characteristics were considered to be of high quality: 1) the acquisition sweep included planes of section from the upper mediastinum and through the upper abdomen; 2) the fetal spine was positioned between 9 and 3 o'clock, minimizing the possibility of shadowing from ribs or spine; and 3) minimum or no motion artifact was observed on the sagittal orthogonal plane to the original plane of acquisition (panel B). Regardless of the perceived quality, at least one volume dataset per patient was included in the study.

Automatic slicing of volume datasets with TUI

Cross-sectional planes to the original plane of acquisition were automatically displayed with TUI, a novel display modality available in version 5.0 of the 4D View Software (General Electric Medical Systems, Kretztechnik, Zipf, Austria) (Figures 1 and 2, video clips 1 and 2). This display modality allows examiners to automatically slice a volume dataset and simultaneously visualize up to eight parallel planes of section on the same screen. Importantly, motion information in volume datasets acquired using 4D ultrasonography techniques is not lost and, therefore, multiple sections of a beating heart can be analyzed at the same time. An "overview image" is shown on the upper left corner. This view depicts a plane orthogonal to the slices, and parallel lines demarcate the position of the slices within the volume dataset (Figure 1). The user can adjust the number and position of the slices with specific software controls. Hue, brightness and contrast controls can also be adjusted to optimize image quality.

Analysis of volume datasets displayed with TUI

All volume datasets were analyzed by a single investigator (LG). Those acquired with B-mode imaging were analyzed first, and visualization rates for cardiac structures in each of the five planes of section proposed by Yagel et al.[73] were determined as follows: 1) abnormal; 2) normal; 3) present in the volume dataset but inadequate for diagnosis; and 4) not present in the volume dataset. To be considered adequate for diagnosis, the following structures and relationships should have been visualized in each scanning plane:

1. Transverse view of the upper abdomen (Figure 1A): 1) stomach on the left side of the abdomen, 2) transverse section of the descending aorta in front and to the left of the spine, 3) inferior vena cava located on the right side of the spine.

2. Four-chamber view: evaluated according to the criteria proposed by the American Institute of Ultrasound in Medicine for the performance of the basic fetal cardiac screening examination (Table 1).[43]
3. Five-chamber view: 1) aortic root visualized and connected to the left ventricle; 2) the anterior wall of the aorta should be in continuity with the ventricular septum. [43]
4. Pulmonary artery view: pulmonary artery visualized leaving the right ventricle and at least one of the branches bifurcating at its distal end.[43,73,75]
5. Three-vessel and trachea view: 1) main pulmonary trunk in direct communication with the ductus arteriosus; 2) transverse section of the aortic arch between the main pulmonary trunk and superior vena cava; 3) cross section of the superior vena cava visualized on the right side of the chest; and 4) trachea visualized posterior to the superior vena cava.[73]

Following the evaluation of B-mode imaging volume datasets, visualization rates for volume datasets acquired with color Doppler were determined according to the criteria proposed by Chaoui and McEwing:[14]

1. Four-chamber view: 1) diastolic perfusion across the AV valves documented with color Doppler, with no evidence of valve regurgitation; 2) no color flow observed crossing the ventricular septum.
2. Five-chamber view: 1) aortic root emerging from the left ventricle; 2) interventricular septum in continuity with the anterior wall of the ascending aorta. Abnormalities in this view included: a) turbulent flow across the aortic valve; b) shunting through a perimembranous VSD with a normal aortic connection; c) visualization of the origin of the pulmonary trunk emerging from the left ventricle identified by its bifurcation into the main pulmonary arteries; and d) overriding of the aorta over both ventricles, connected by a VSD.
3. Three-vessel view: 1) aorta and pulmonary trunk converging toward the left thorax with the trachea to their right; 2) pulmonary trunk with a slightly greater caliber than the aorta (ratio 1.2:1); 3) straight course of the vessels; and 4) antegrade flow through both great vessels throughout the cardiac cycle.

Volume datasets acquired with B-mode imaging and color Doppler were compared to determine if color Doppler provided more information than that obtained by examination with B-mode imaging alone. Visualization rates for the four- and five-chamber and three-vessel views were compared using the McNemar's test. Agreement between diagnoses by the two-modalities was tested using the Kappa test.

Following determination of the visualization rates for each view, the diagnoses established by TUI were compared to postnatal diagnoses by neonatal imaging modalities, cardiac surgery or autopsy. Sensitivity, specificity, as well as positive- and negative-predictive values for the diagnosis of congenital heart disease were calculated first for volume datasets acquired with B-mode imaging and then for those acquired with the addition of color Doppler. Cases of isolated VSDs (either suspected prenatally or detected in the neonatal period) were excluded from this analysis because neonatal echocardiograms are not performed in every neonate in our institution in the absence of symptoms.

Statistical analysis was performed with SPSS 12.0 for Windows (SPSS, Chicago, IL).

Results

STIC volume datasets of the fetal heart were acquired with B-mode or color Doppler imaging in 195 and 168 cases, respectively.

Table II shows visualization rates for anatomical structures expected to be present in the five transverse scanning planes proposed by Yagel et al.,[73] after automatic slicing with TUI (Figure 1, video clip 1). The four- and five-chamber and three-vessel and trachea views were visualized in 97.4% (190/195), 88.2% (172/195), and 79.5% (142/195) of the cases, respectively. A three-vessel view showing bifurcation of the pulmonary artery was visualized in only 51.8% (101/195) of the cases. Transverse views of the upper fetal abdomen were present in 64.1% of the volume datasets (125/195).

In volume datasets acquired with color Doppler (Figure 2,), the four- and five-chamber and three-vessel views were visualized in 98.2% (165/168), 97.0% (163/168), and 83.6% (145/168) of the cases, respectively (Table III). Table IV compares the visualization rates for the four-chamber, five-chamber and three-vessel views between volume datasets acquired with B-mode or color Doppler imaging. The additional contribution of color Doppler imaging was statistically significant for the five-chamber view only (McNemar test = 13.5, $p = 0.004$).

Isolated VSDs were suspected in 19 cases with B-mode imaging and 23 cases when the examination was performed with color Doppler. When isolated VSDs were excluded from the analysis, congenital heart anomalies were identified by TUI in 16 of the 195 fetuses (8.2%) (Table V). Figures 3, 4, 5 and 6 (video clips 3, 4, 5 and 6) illustrate abnormal findings in the various planes of sections displayed by TUI in cases of coarctation of the aorta, hypoplastic left heart, pulmonary atresia and transposition of the great arteries. Color Doppler provided additional diagnostic information in 5 of the 16 cases (31.3%). In case 5, retrograde perfusion of the pulmonary artery helped to correctly diagnose pulmonary atresia in a case of hypoplastic right ventricle (Figure 5). In case 6, a VSD was demonstrated in association with coarctation of the aorta. In case 8, disproportion in size between the right and left ventricles observed by B-mode imaging was correctly diagnosed as coarctation of the aorta (Figure 3). In case 13, color Doppler allowed the visualization of an interrupted IVC with azygous continuation in a case where volume datasets acquired by B-mode imaging were considered non-diagnostic. In case 16, what was initially suspected as transposition of the great arteries was diagnosed as tetralogy of Fallot.

Table VI compares diagnoses established by the review of volume datasets displayed with TUI and postnatal diagnoses (isolated VSDs were excluded). Among the 17 cases with a cardiac anomaly suspected by TUI or identified in the neonatal period, two were lost to follow-up. In one case, only a fetal echocardiogram performed by an independent pediatric cardiologist was available for comparison. Among the 15 patients for whom follow-up was available, there was perfect agreement between prenatal and postnatal diagnoses in 73.3% of the cases (11/15). The four discrepant diagnoses were: 1) in case 3, a fetus diagnosed with tetralogy of Fallot by TUI had a postnatal diagnosis of TGA associated with a subaortic VSD; 2) in case 7, coarctation of the aorta was suspected by both B-mode and color Doppler but was not confirmed in the neonate; 3) in case 10, a rhabdomioma was not visualized by both B-mode and color Doppler volume datasets displayed with TUI; and 4) in case 14, severe tricuspid regurgitation was detected in a fetus whose final diagnosis was Ebstein anomaly.

Sensitivity, specificity, positive- and negative-predictive values of TUI for the diagnosis of congenital heart disease, excluding cases of isolated VSDs, are displayed in Table VII. For this analysis, cases 3 and 14 (Table VI) were considered as true positive diagnoses because, although a specific diagnosis was not made, a significant cardiac anomaly was suspected by TUI.

Among fetuses with a VSD suspected by B-mode imaging and color Doppler (n=23), two cases (8.7%) were confirmed after delivery, one case (4.3%) was diagnosed as an AV canal, and another (4.3%) case was diagnosed as double inlet single ventricle. One of the three (33.3%) isolated VSDs detected after delivery was missed by prenatal examination of STIC volume datasets displayed with TUI.

Discussion

The results of this study indicate that: 1) the four-and five-chamber and three-vessel and trachea views can be visualized in the majority of volume datasets automatically sliced with TUI; 2) color Doppler provides additional diagnostic information in 10% of the three-vessel views, 12% of the four-chamber views, and 14% of the five-chamber views displayed with this modality; 3) the additional information provided by color Doppler helped to establish a correct diagnosis in 31% of the fetuses with cardiac anomalies other than isolated VSDs; and 4) the diagnoses established by TUI agreed with the postnatal diagnoses in 73.3% of the fetuses, with good sensitivity, specificity, positive- and negative-predictive values for the diagnosis of congenital heart disease.

Technical aspects of 4D ultrasonography with STIC have been described by several investigators. [8,13,21–24,28–30,32,33,71,72,74] However, a systematic evaluation of the capability of obtaining specific planes of section with this diagnostic modality has been reported once.[72] Viñals et al.[72] studied 100 fetuses who were examined by 4D ultrasonography with STIC, and whose volume datasets were evaluated by a specialist in fetal echocardiography who was not involved in volume acquisition. Standard cardiac planes were obtained by scrolling through the volume datasets from the upper abdomen to the mediastinum. Visualization rates for the four-chamber view, left and right ventricular outflow tracts, three-vessel view, and three-vessel and trachea views ranged from 81 to 100%, with the lowest visualization rates observed for structures located in the abdomen or upper mediastinum. TUI provides an alternative approach to manually scrolling through the volume datasets to obtain these cardiac views. The difference between the two approaches is that the volume dataset is automatically sliced and, thus, it comes as no surprise to us that the visualization rates for cardiac structures reported by Viñals et al. [72] are similar to those reported in the current study.

The view with the poorest visualization rates in our study was the three-vessel view demonstrating bifurcation of the main pulmonary artery, the fourth plane of section proposed by Yagel et al.[73] This could reflect the short distance between this plane and the three-vessel and trachea view. Therefore, visualization of both planes using automatic slicing techniques with a fixed distance between the planes of section may have forced the display of one plane to the detriment of the other. Although the distance between each slice can be adjusted by the software and thus potentially correct this problem, we wanted to evaluate how this new technique would perform with minimum operator interference. It is important, however, to be aware of this limitation, since if this view is not automatically displayed, the examiner may need to use other techniques to explore the volume dataset in order to visualize the pulmonary artery and its bifurcation. Among these techniques, the examiner may choose to use a previously reported systematic approach for evaluation of the outflow tracts with STIC,[31, 32] whereby both the long axis view of the left ventricular outflow tract and the short axis view of the right outflow tract are displayed side-by-side on the same image, the “spin” technique reported by DeVore et al.,[22] or rendering techniques to visualize the relationship between both great arteries on the same image.[13,24,28,29,33]

The results of this study also corroborate the proposal of Chaoui and McEwing[14] that the examination of three-planes of section (four- and five-chamber and three-vessel views) with

color Doppler may be sufficient to detect most cases of congenital heart disease. Indeed, these investigators subsequently reported that these three planes could be demonstrated in 31/35 healthy fetuses and in 24/27 fetuses with CHD in volume datasets acquired with color Doppler STIC.[13] In the current study, the four- and five-chamber and three-vessel views acquired with color Doppler were visualized in 98.2%, 97.0%, and 83.6% of the cases, respectively, and additional diagnostic information was observed in 12%, 14% and 10% of these views when compared to B-mode imaging only. More importantly, color Doppler helped to establish the correct diagnosis of pulmonary atresia and coarctation of the aorta in two cases in which the previous findings by B-mode imaging had shown only disproportional ventricular size.

The role of sonographic tomography in clinical practice remains to be determined. Benacerraf et al.[6] reported preliminary findings in 25 pregnancies scanned during the second trimester, in which five volume datasets encompassing the fetal head, face, chest, abdomen, and limbs were acquired for offline later analysis. Volume datasets were examined by physicians who were not involved in volume acquisition, and the visualization rates for fetal anatomical structures and time to complete the examination (including volume acquisition and review) were calculated. Complete structural surveys were obtained in 20 of the 25 fetuses. In one of the 5 incomplete surveys, a face was visualized by neither 3D nor 2D ultrasound. Portions of the hands and feet were not visualized in the other four cases. Importantly, the time required to complete the anatomical surveys was decreased by half using 3D ultrasonography (13.9 minutes vs. 6.6 minutes, $p<0.001$). With the availability of software to automatically slice the volume datasets, busy clinical practices may welcome this approach.

Leung et al.[44] have recently reported the use of automatic slicing of 3D volume datasets (Multi-Slice View, Accuvix, Medison, Seoul, Korea) for the examination of the fetal spine, face, brain and heart in a group of 35 fetuses scanned during the second trimester of pregnancy, and demonstrated the feasibility of diagnosing neural tube defects, facial clefts, and holoprosencephaly. The current study extends these observations to prenatal diagnosis of congenital heart disease. Although most cases of congenital heart disease other than VSDs were correctly diagnosed by exploring the volume datasets with the novel TUI display, this portion of our study needs to be interpreted with caution. Despite removing patient identifiers and including only cases examined at least 6 months before the conduction of this study, the possibility of recall bias exists. Therefore, our results need to be independently confirmed.

Supplementary Material

Refer to Web version on PubMed Central for supplementary material.

Acknowledgements

This research was supported by the Intramural Research Program of the National Institute of Child Health and Human Development, NIH, DHHS.

References

1. Abuhamad A. Automated multiplanar imaging: a novel approach to ultrasonography. J Ultrasound Med 2004;23:573. [PubMed: 15154522]
2. Acar P, Dulac Y, Taktak A, Villaceque M. [Real time 3D echocardiography in congenital heart disease]. Arch Mal Coeur Vaiss 2004;97:472. [PubMed: 15214550]
3. Allan L, Benacerraf B, Copel JA, Carvalho JS, Chaoui R, Eik-Nes SH, Tegnander E, Gembruch U, Huhta JC, Pilu G, Wladimiroff J, Yagel S. Isolated major congenital heart disease. Ultrasound Obstet Gynecol 2001;17:370. [PubMed: 11380959]
4. Arzt W, Tulzer G, Aigner M. [Real time 3D sonography of the normal fetal heart--clinical evaluation]. Ultraschall Med 2002;23:388. [PubMed: 12514755]

5. Bega G, Kuhlman K, Lev-Toaff A, Kurtz A, Wapner R. Application of three-dimensional ultrasonography in the evaluation of the fetal heart. J Ultrasound Med 2001;20:307. [PubMed: 11316308]
6. Benacerraf BR, Shipp TD, Bromley B. How sonographic tomography will change the face of obstetric sonography: a pilot study. J Ultrasound Med 2005;24:371. [PubMed: 15723850]
7. Bhat AH, Corbett V, Carpenter N, Liu N, Liu R, Wu A, Hopkins G, Sohaey R, Winkler C, Sahn CS, Sovinsky V, Li X, Sahn DJ. Fetal ventricular mass determination on three-dimensional echocardiography: studies in normal fetuses and validation experiments. Circulation 2004;110:1054. [PubMed: 15326076]
8. Bhat AH, Corbett VN, Liu R, Carpenter ND, Liu NW, Wu AM, Hopkins GD, Li X, Sahn DJ. Validation of volume and mass assessments for human fetal heart imaging by 4-dimensional spatiotemporal image correlation echocardiography: in vitro balloon model experiments. J Ultrasound Med 2004;23:1151. [PubMed: 15328429]
9. Bonnet D, Coltri A, Butera G, Fermont L, Le Bidois J, Kachaner J, Sidi D. Detection of transposition of the great arteries in fetuses reduces neonatal morbidity and mortality. Circulation 1999;99:916. [PubMed: 10027815]
10. Brekke S, Tegnander E, Torp HG, Eik-Nes SH. Tissue Doppler gated (TDOG) dynamic three-dimensional ultrasound imaging of the fetal heart. Ultrasound Obstet Gynecol 2004;24:192. [PubMed: 15287059]
11. Buskens E, Grobbee DE, Frohn-Mulder IME, Stewart PA, Juttmann RE, Wladimiroff JW, Hess J. Efficacy of Routine Fetal Ultrasound Screening for Congenital Heart Disease in Normal Pregnancy. Circulation 1996;94:67. [PubMed: 8964120]
12. Chang FM, Hsu KF, Ko HC, Yao BL, Chang CH, Yu CH, Liang RI, Chen HY. Fetal heart volume assessment by three-dimensional ultrasound. Ultrasound Obstet Gynecol 1997;9:42. [PubMed: 9060130]
13. Chaoui R, Hoffmann J, Heling KS. Three-dimensional (3D) and 4D color Doppler fetal echocardiography using spatio-temporal image correlation (STIC). Ultrasound Obstet Gynecol 2004;23:535. [PubMed: 15170792]
14. Chaoui R, McEwing R. Three cross-sectional planes for fetal color Doppler echocardiography. Ultrasound Obstet Gynecol 2003;21:81. [PubMed: 12528169]
15. Crane JP, LeFevre ML, Winborn RC, Evans JK, Ewigman BG, Bain RP, Frigoletto FD, McNellis D. A randomized trial of prenatal ultrasonographic screening: impact on the detection, management, and outcome of anomalous fetuses. The RADIUS Study Group. Am J Obstet Gynecol 1994;171:392. [PubMed: 8059817]
16. Deng J, Gardener JE, Rodeck CH, Lees WR. Fetal echocardiography in three and four dimensions. Ultrasound Med Biol 1996;22:979. [PubMed: 9004421]
17. Deng J, Richards R. Dynamic three-dimensional gray-scale and color Doppler ultrasound of the fetal heart for dynamic diagnosis. Ultrasound Obstet Gynecol 2002;20:209. [PubMed: 12153679]
18. Deng J, Sullivan ID, Yates R, Vogel M, Mcdonald D, Linney AD, Rodeck CH, Anderson RH. Real-time three-dimensional fetal echocardiography--optimal imaging windows. Ultrasound Med Biol 2002;28:1099. [PubMed: 12401378]
19. Deng J, Yates R, Birkett AG, Ruff CF, Linney AD, Lees WR, Hanson MA, Rodeck CH. Online motion-gated dynamic three-dimensional echocardiography in the fetus--preliminary results. Ultrasound Med Biol 2001;27:43. [PubMed: 11295269]
20. Deng J, Yates R, Sullivan ID, Mcdonald D, Linney AD, Lees WR, Anderson RH, Rodeck CH. Dynamic three-dimensional color Doppler ultrasound of human fetal intracardiac flow. Ultrasound Obstet Gynecol 2002;20:131. [PubMed: 12153663]
21. DeVore GR, Falkensammer P, Sklansky MS, Platt LD. Spatio-temporal image correlation (STIC): new technology for evaluation of the fetal heart. Ultrasound Obstet Gynecol 2003;22:380. [PubMed: 14528474]
22. DeVore GR, Polanco B, Sklansky MS, Platt LD. The ‘spin’ technique: a new method for examination of the fetal outflow tracts using three-dimensional ultrasound. Ultrasound Obstet Gynecol 2004;24:72. [PubMed: 15229920]

23. Espinoza J, Goncalves LF, Lee W, Chaiworapongsa T, Treadwell MC, Stites S, Schoen ML, Mazor M, Romero R. The use of the minimum projection mode in 4-dimensional examination of the fetal heart with spatiotemporal image correlation. J Ultrasound Med 2004;23:1337. [PubMed: 15448324]
24. Espinoza J, Goncalves LF, Lee W, Mazor M, Romero R. A novel method to improve prenatal diagnosis of abnormal systemic venous connections using three- and four-dimensional ultrasonography and 'inversion mode'. Ultrasound Obstet Gynecol 2005;25:428. [PubMed: 15846761]
25. Fernandez CO, Ramaciotti C, Martin LB, Twickler DM. The four-chamber view and its sensitivity in detecting congenital heart defects. Cardiology 1998;90:202. [PubMed: 9892769]
26. Franklin O, Burch M, Manning N, Sleeman K, Gould S, Archer N. Prenatal diagnosis of coarctation of the aorta improves survival and reduces morbidity. Heart 2002;87:67. [PubMed: 11751670]
27. Garne E, Stoll C, Clementi M. Evaluation of prenatal diagnosis of congenital heart diseases by ultrasound: experience from 20 European registries. Ultrasound Obstet Gynecol 2001;17:386. [PubMed: 11380961]
28. Goncalves LF, Espinoza J, Lee W, Mazor M, Romero R. Three- and four-dimensional reconstruction of the aortic and ductal arches using inversion mode: a new rendering algorithm for visualization of fluid-filled anatomical structures. Ultrasound Obstet Gynecol 2004;24:696. [PubMed: 15521086]
29. Goncalves LF, Espinoza J, Lee W, Nien JK, Hong JS, Santolaya-Forgas J, Mazor M, Romero R. A new approach to fetal echocardiography: digital casts of the fetal cardiac chambers and great vessels for detection of congenital heart disease. J Ultrasound Med 2005;24:415. [PubMed: 15784759]
30. Goncalves LF, Espinoza J, Romero R, Lee W, Beyer B, Treadwell MC, Humes R. A systematic approach to prenatal diagnosis of transposition of the great arteries using 4-dimensional ultrasonography with spatiotemporal image correlation. J Ultrasound Med 2004;23:1225. [PubMed: 15328439]
31. Goncalves LF, Espinoza J, Romero R, Lee W, Treadwell M, Huang SE, DeVore GR, Chaiworapongsa T, Schoen ML. Four-dimensional fetal echocardiography with spatiotemporal image correlation (STIC): a systematic study of standard cardiac views assessed by different observers. J Matern Fetal Neonatal Med 2005;18in press
32. Goncalves LF, Lee W, Chaiworapongsa T, Espinoza J, Schoen ML, Falkensammer P, Treadwell M, Romero R. Four-dimensional ultrasonography of the fetal heart with spatiotemporal image correlation. Am J Obstet Gynecol 2003;189:1792. [PubMed: 14710117]
33. Goncalves LF, Romero R, Espinoza J, Lee W, Treadwell M, Chintala K, Brandl H, Chaiworapongsa T. Four-dimensional ultrasonography of the fetal heart using color Doppler spatiotemporal image correlation. J Ultrasound Med 2004;23:473. [PubMed: 15098864]
34. Grandjean H, Larroque D, Levi S. The performance of routine ultrasonographic screening of pregnancies in the Eurofetus Study. Am J Obstet Gynecol 1999;181:446. [PubMed: 10454699]
35. Guerra FA, Isla AI, Aguilar RC, Fritz EG. Use of free-hand three-dimensional ultrasound software in the study of the fetal heart. Ultrasound Obstet Gynecol 2000;16:329. [PubMed: 11169308]
36. Herberg U, Goldberg H, Breuer J. Dynamic free-hand three-dimensional fetal echocardiography gated by cardiotocography. Ultrasound Obstet Gynecol 2003;22:493. [PubMed: 14618663]
37. Herberg U, Goldberg H, Breuer J. Three- and four-dimensional freehand fetal echocardiography: a feasibility study using a hand-held Doppler probe for cardiac gating. Ultrasound Obstet Gynecol 2005;25:362. [PubMed: 15761914]
38. Hoffman JI, Kaplan S. The incidence of congenital heart disease. J Am Coll Cardiol 2002;39:1890. [PubMed: 12084585]
39. Hoffman JIE, Christianson R. Congenital heart disease in a cohort of 19,502 births with long-term follow-up. The American Journal of Cardiology 1978;42:641. [PubMed: 696646]
40. Jaeggi ET, Sholler GF, Jones OD, Cooper SG. Comparative analysis of pattern, management and outcome of pre- versus postnatally diagnosed major congenital heart disease: a population-based study. Ultrasound Obstet Gynecol 2001;17:380. [PubMed: 11380960]
41. Jurgens J, Chaoui R. Three-dimensional multiplanar time-motion ultrasound or anatomical M-mode of the fetal heart: a new technique in fetal echocardiography. Ultrasound Obstet Gynecol 2003;21:119. [PubMed: 12601830]

42. Klein SK, Cans C, Robert E, Jouk PS. Efficacy of routine fetal ultrasound screening for congenital heart disease in Isere County, France. Prenat Diagn 1999;19:318. [PubMed: 10327135]
43. Lee W. Performance of the basic fetal cardiac ultrasound examination. Journal Of Ultrasound In Medicine: Official Journal Of The American Institute Of Ultrasound In Medicine 1998;17:601. [PubMed: 9733183]
44. Leung KY, Ngai CS, Chan BC, Leung WC, Lee CP, Tang MH. Three-dimensional extended imaging: a new display modality for three-dimensional ultrasound examination. Ultrasound Obstet Gynecol 2005;26:244. [PubMed: 16116563]
45. Levental M, Pretorius DH, Sklansky MS, Budorick NE, Nelson TR, Lou K. Three-dimensional ultrasonography of normal fetal heart: comparison with two-dimensional imaging. J Ultrasound Med 1998;17:341. [PubMed: 9623470]
46. Levi S, Cos-Sanchez T. [Fetal echocardiography volume mode (3 dimensions)]. J Gynecol Obstet Biol Reprod (Paris) 2000;29:261. [PubMed: 10804367]
47. Mahle WT, Clancy RR, McGaurn SP, Goin JE, Clark BJ. Impact of prenatal diagnosis on survival and early neurologic morbidity in neonates with the hypoplastic left heart syndrome. Pediatrics 2001;107:1277. [PubMed: 11389243]
48. Maulik D, Nanda NC, Singh V, Dod H, Vengala S, Sinha A, Sidhu MS, Khanna D, Lysikiewicz A, Sicuranza G, Modh N. Live three-dimensional echocardiography of the human fetus. Echocardiography 2003;20:715. [PubMed: 14641376]
49. Meyer-Wittkopf M, Cole A, Cooper SG, Schmidt S, Sholler GF. Three-dimensional quantitative echocardiographic assessment of ventricular volume in healthy human fetuses and in fetuses with congenital heart disease. J Ultrasound Med 2001;20:317. [PubMed: 11316309]
50. Meyer-Wittkopf M, Cook A, McLennan A, Summers P, Sharland GK, Maxwell DJ. Evaluation of three-dimensional ultrasonography and magnetic resonance imaging in assessment of congenital heart anomalies in fetal cardiac specimens. Ultrasound Obstet Gynecol 1996;8:303. [PubMed: 8978001]
51. Meyer-Wittkopf M, Cooper S, Vaughan J, Sholler G. Three-dimensional (3D) echocardiographic analysis of congenital heart disease in the fetus: comparison with cross-sectional (2D) fetal echocardiography. Ultrasound Obstet Gynecol 2001;17:485. [PubMed: 11422968]
52. Meyer-Wittkopf M, Hofbeck M. [Two- and three-dimensional echocardiographic analysis of congenital heart disease in the fetus]. Herz 2003;28:240. [PubMed: 12756481]
53. Meyer-Wittkopf M, Rappe N, Sierra F, Barth H, Schmidt S. Three-dimensional (3-D) ultrasonography for obtaining the four and five-chamber view: comparison with cross-sectional (2-D) fetal sonographic screening. Ultrasound Obstet Gynecol 2000;15:397. [PubMed: 10976481]
54. Michailidis GD, Simpson JM, Karidas C, Economides DL. Detailed three-dimensional fetal echocardiography facilitated by an Internet link. Ultrasound Obstet Gynecol 2001;18:325. [PubMed: 11778990]
55. Nelson TR. Three-dimensional fetal echocardiography. Prog Biophys Mol Biol 1998;69:257. [PubMed: 9785942]
56. Nelson TR, Pretorius DH, Sklansky M, Hagen-Ansert S. Three-dimensional echocardiographic evaluation of fetal heart anatomy and function: acquisition, analysis, and display. J Ultrasound Med 1996;15:1. [PubMed: 8667477]
57. Roguin N, Du ZD, Barak M, Nasser N, Hershkowitz S, Milgram E. High prevalence of muscular ventricular septal defect in neonates. Journal of the American College of Cardiology 1995;26:1545. [PubMed: 7594083]
58. Rustico MA, Benettoni A, D'Ottavio G, Maieron A, Fischer-Tamaro I, Conoscenti G, Meir Y, Montesano M, Cattaneo A, Mandruzzato G. Fetal heart screening in low-risk pregnancies. Ultrasound Obstet Gynecol 1995;6:313. [PubMed: 8590200]
59. Sands AJ, Casey FA, Craig BG, Dornan JC, Rogers J, Mulholland HC. Incidence and risk factors for ventricular septal defect in "low risk" neonates. Arch Dis Child Fetal Neonatal Ed 1999;81:F61. [PubMed: 10375365]
60. Scharf A, Geka F, Steinborn A, Frey H, Schlemmer A, Sohn C. 3D real-time imaging of the fetal heart. Fetal Diagn Ther 2000;15:267. [PubMed: 10971079]

61. Sklansky M. New dimensions and directions in fetal cardiology. Curr Opin Pediatr 2003;15:463. [PubMed: 14508293]
62. Sklansky MS, DeVore GR, Wong PC. Real-time 3-dimensional fetal echocardiography with an instantaneous volume-rendered display: early description and pictorial essay. J Ultrasound Med 2004;23:283. [PubMed: 14992367]
63. Sklansky MS, Nelson T, Strachan M, Pretorius D. Real-time three-dimensional fetal echocardiography: initial feasibility study. J Ultrasound Med 1999;18:745. [PubMed: 10547106]
64. Sklansky MS, Nelson TR, Pretorius DH. Usefulness of gated three-dimensional fetal echocardiography to reconstruct and display structures not visualized with two-dimensional imaging. Am J Cardiol 1997;80:665. [PubMed: 9295008]
65. Sklansky MS, Nelson TR, Pretorius DH. Three-dimensional fetal echocardiography: gated versus nongated techniques. J Ultrasound Med 1998;17:451. [PubMed: 9669304]
66. Stoll C, Alembik Y, Dott B, Meyer MJ, Pennerath A, Peter MO, De Geeter B. Evaluation of prenatal diagnosis of congenital heart disease. Prenat Diagn 1998;18:801. [PubMed: 9742567]
67. Stoll C, Alembik Y, Dott B, Roth PM, De Geeter B. Evaluation of prenatal diagnosis of congenital heart disease. Prenat Diagn 1993;13:453. [PubMed: 8372071]
68. Tegnander E, Eik-Nes SH. The examiner's ultrasound experience has a significant impact on the detection rate of congenital heart defects at the second trimester fetal examination [abstract]. Ultrasound Obstet Gynecol 2004;24:217. [PubMed: 15329970]
69. Todros T, Faggiano F, Chiappa E, Gaglioti P, Mitola B, Sciarrone A. Accuracy of routine ultrasonography in screening heart disease prenatally. Gruppo Piemontese for Prenatal Screening of Congenital Heart Disease. Prenat Diagn 1997;17:901. [PubMed: 9358568]
70. Tworetzky W, McElhinney DB, Reddy VM, Brook MM, Hanley FL, Silverman NH. Improved surgical outcome after fetal diagnosis of hypoplastic left heart syndrome. Circulation 2001;103:1269. [PubMed: 11238272]
71. Vinals F, Mandujano L, Vargas G, Giuliano A. Prenatal diagnosis of congenital heart disease using four-dimensional spatio-temporal image correlation (STIC) telemedicine via an Internet link: a pilot study. Ultrasound Obstet Gynecol 2005;25:25. [PubMed: 15593355]
72. Vinals F, Poblete P, Giuliano A. Spatio-temporal image correlation (STIC): a new tool for the prenatal screening of congenital heart defects. Ultrasound Obstet Gynecol 2003;22:388. [PubMed: 14528475]
73. Yagel S, Arbel R, Anteby EY, Raveh D, Achiron R. The three vessels and trachea view (3VT) in fetal cardiac scanning. Ultrasound Obstet Gynecol 2002;20:340. [PubMed: 12383314]
74. Yagel S, Valsky DV, Messing B. Detailed assessment of fetal ventricular septal defect with 4D color Doppler ultrasound using spatio-temporal image correlation technology. Ultrasound Obstet Gynecol 2005;25:97. [PubMed: 15690557]
75. Yoo SJ, Lee YH, Kim ES, Ryu HM, Kim MY, Choi HK, Cho KS, Kim A. Three-vessel view of the fetal upper mediastinum: an easy means of detecting abnormalities of the ventricular outflow tracts and great arteries during obstetric screening. Ultrasound Obstet Gynecol 1997;9:173. [PubMed: 9165680]
76. Zosmer N, Jurkovic D, Jauniaux E, Gruboeck K, Lees C, Campbell S. Selection and identification of standard cardiac views from three-dimensional volume scans of the fetal thorax. J Ultrasound Med 1996;15:25. [PubMed: 8667480]

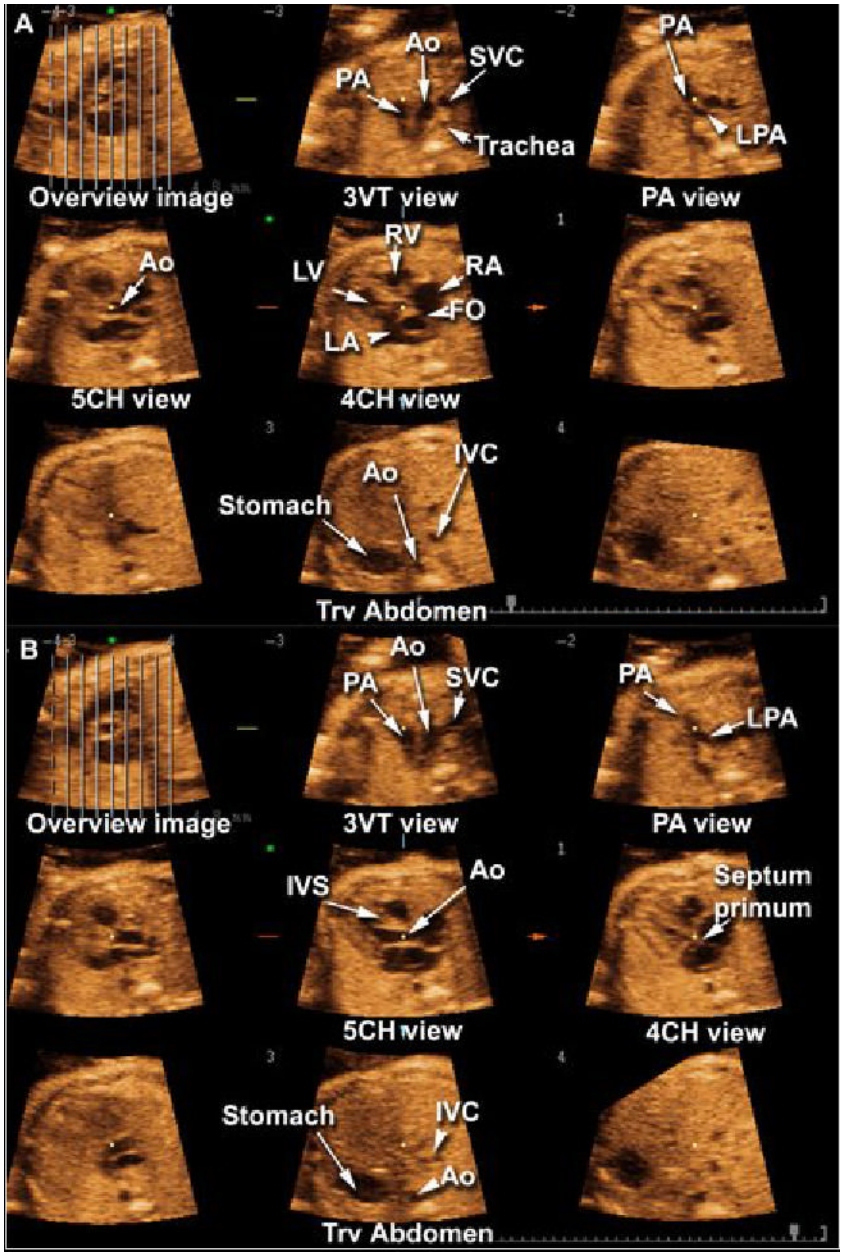

Figure 1.

Tomographic Ultrasound Imaging of a normal fetal heart in systole (A) and diastole (B). The overview image on the left upper panel of each figure shows the orthogonal sagittal plane to the sections that are being displayed. Each line represents a slice. The center slice is marked with an asterisk (*) and each subsequent plane to the right or left is marked with numbers ranging from −4 to +4. The plane marked by the dotted line is not displayed. In this volume dataset, the five transverse planes of section proposed by Yagel et al. (Ultrasound Obstet Gynecol 2001;17:367–369) for the examination of the fetal heart are visualized. Please note that the five chamber view was better visualized during systole. Legends: PA: pulmonary artery; Ao: aorta; SVC: superior vena cava; LPA: left pulmonary artery; RV: right ventricle; LV: left ventricle; RA: right atrium; LA: left atrium; FO: foramen ovale; IVC: inferior vena cava; IVS: interventricular septum; 4CH: four-chamber; 5CH: five-chamber.

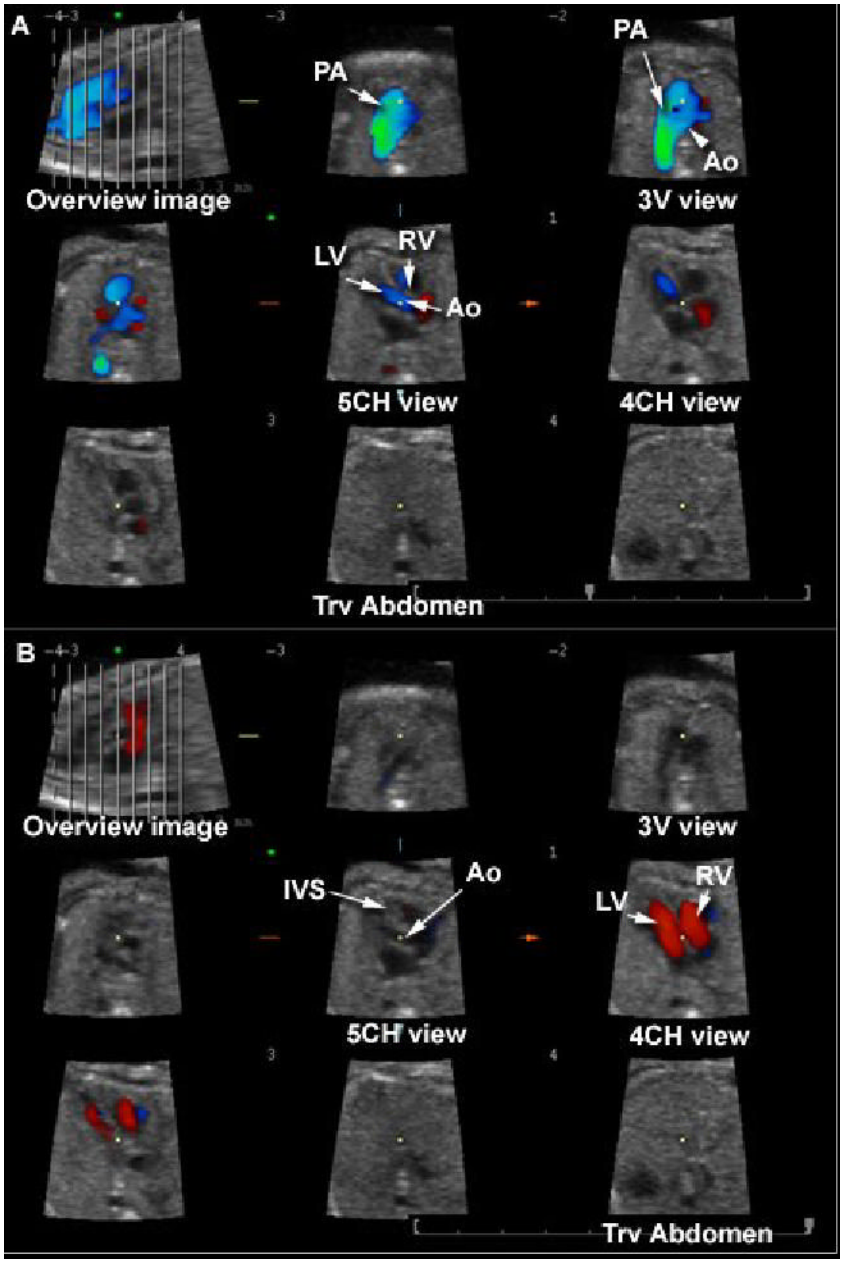

Figure 2.

Tomographic Ultrasound Imaging (TUI) of a normal fetal heart in systole (A) and diastole (B). The volume datasets were acquired using B-mode and color Doppler imaging. The overview image on the left upper panel of each figure shows the orthogonal sagittal plane to the sections that are being displayed. Each line represents a slice. The center slice is marked with an asterisk (*) and each subsequent plane to the right or left are marked with numbers ranging from −4 to +4. The plane marked by the dotted line is not displayed. In this volume dataset, the three planes of section proposed by Chaoui et al. (Ultrasound Obstet Gynecol 2003;21:81–93) for the examination of the fetal heart are visualized.. Legends: PA: pulmonary artery; Ao: aorta; RV: right ventricle; LV: left ventricle; IVS: interventricular septum; 4CH: four-chamber; 5CH: five-chamber.

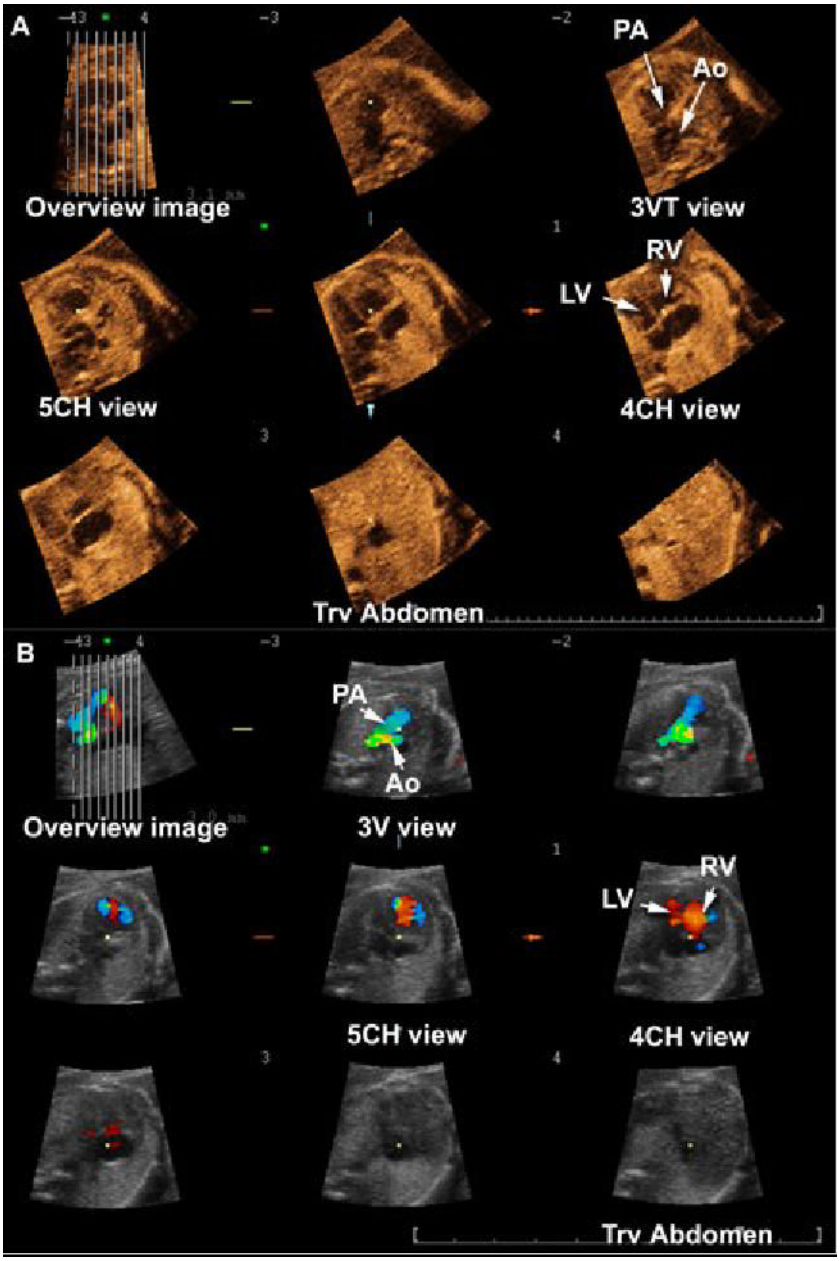

Figure 3.

Tomographic Ultrasound Imaging of a fetus with coarctation of the aorta. A) Volume dataset acquired with B-mode: (1) the three-vessel and trachea view shows a narrow transverse section of the aortic arch; (2) the four-chamber view shows disproportion between the right and left ventricles. B) Volume dataset acquired with color Doppler: (1) the three vessel view confirms the narrow transverse aortic arch and shows aliasing; (2) disproportion between the right and left ventricles is confirmed in the 4-chamber view. Legends: PA = pulmonary artery; Ao = aorta; RV = right ventricle; LV = left ventricle; 3V = three vessel; 3VT = three-vessel and trachea; 4CH = four-chamber; 5CH = five-chamber; Trv = transverse.

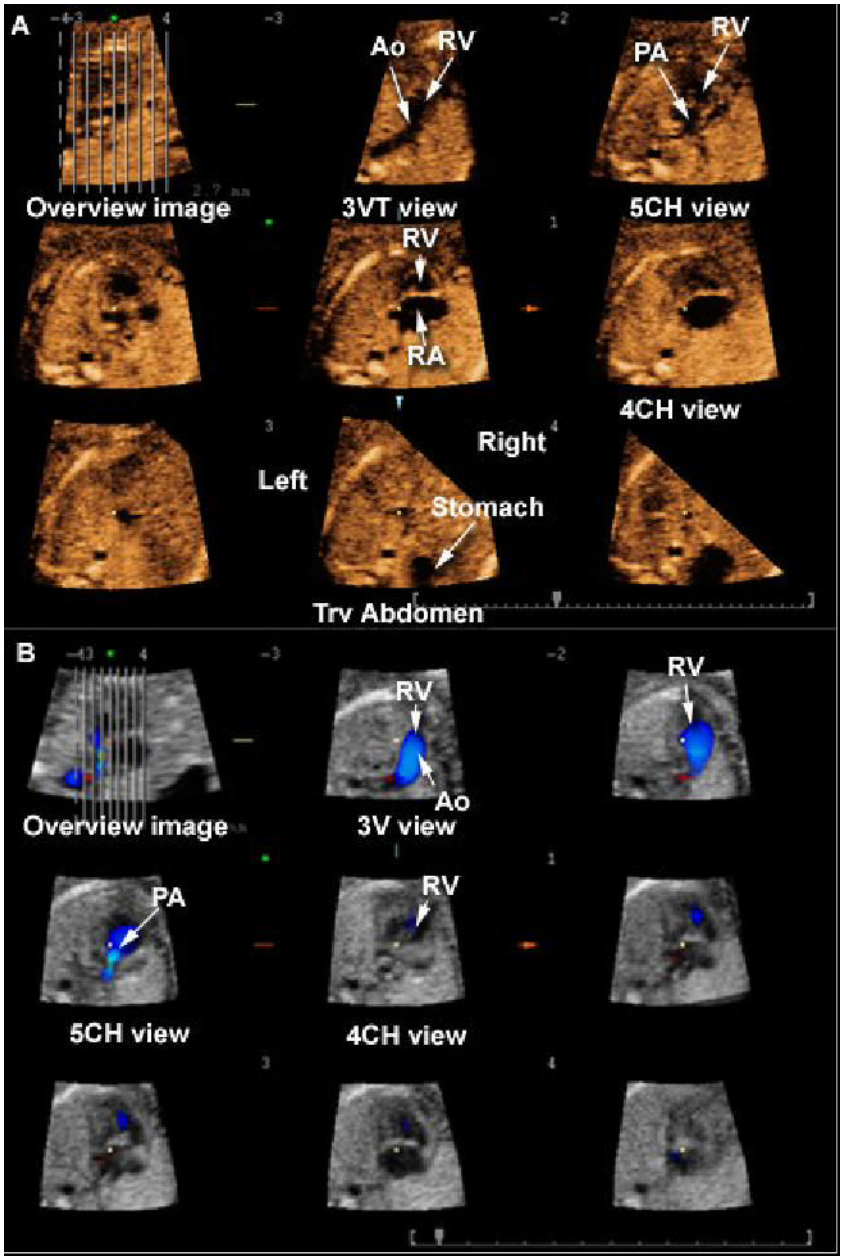

Figure 4.

Tomographic Ultrasound Imaging of a fetus with hypoplastic left heart syndrome, double outlet right ventricle and transposition of the great arteries. A) Volume dataset acquired with B-mode: (1) the three-vessel and trachea view shows the aorta leaving the right ventricle; (2) the five-chamber view shows the pulmonary artery leaving the right ventricle as well; (3) the four-chamber view shows the right ventricle and atrium only – the left ventricle is not visualized; 4) the transverse view of the fetal abdomen shows that the stomach is located on the right. B) Bolume dataset acquired with color Doppler: (1) the three-vessel view confirms that the aorta leaves the right ventricle; (2) the five-chamber view shows the pulmonary artery leaving the right ventricle as well. Legends: PA = pulmonary artery; Ao = aorta; RV = right ventricle; LV = left ventricle; 3V = three vessel; 3VT = three-vessel and trachea; 4CH = four-chamber; 5CH = five-chamber; Trv = transverse.

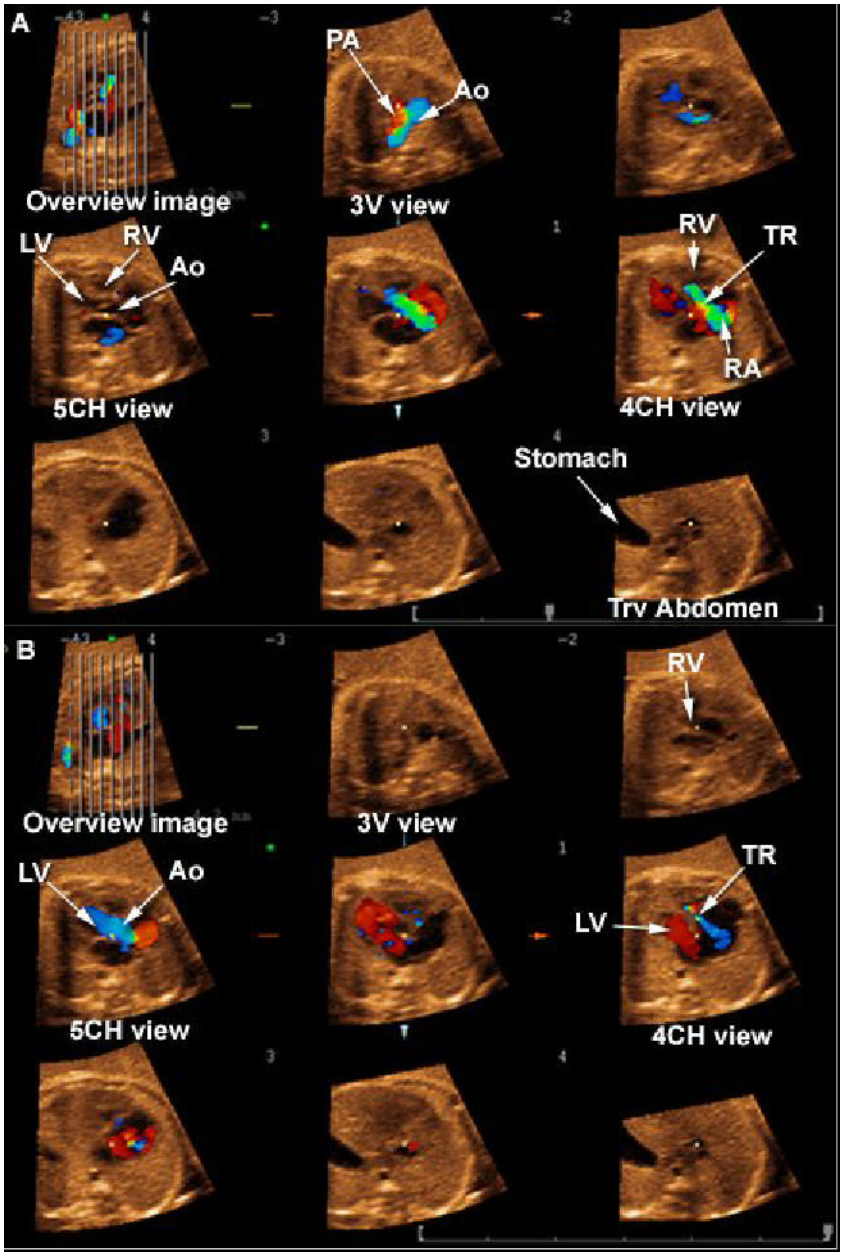

Figure 5.

Tomographic Ultrasound Imaging in a fetus with pulmonary atresia. A) Systole. (1) In the three-vessel view, retrograde perfusion (in red) of a narrow pulmonary artery is observed; (2) severe tricuspid regurgitation is observed in the four-chamber view. B) Diastole: (1) the 5-chamber view shows the aorta connecting normally to the left ventricle; (2) the four-chamber view shows normal ventricular filling only on the left ventricle, with tricuspid regurgitation still observed in blue. Legends: PA = pulmonary artery; Ao = aorta; RV = right ventricle; LV = left ventricle; 3V = three vessel; 4CH = four-chamber; 5CH = five-chamber; Trv = transverse; TR: tricuspid regurgitation.

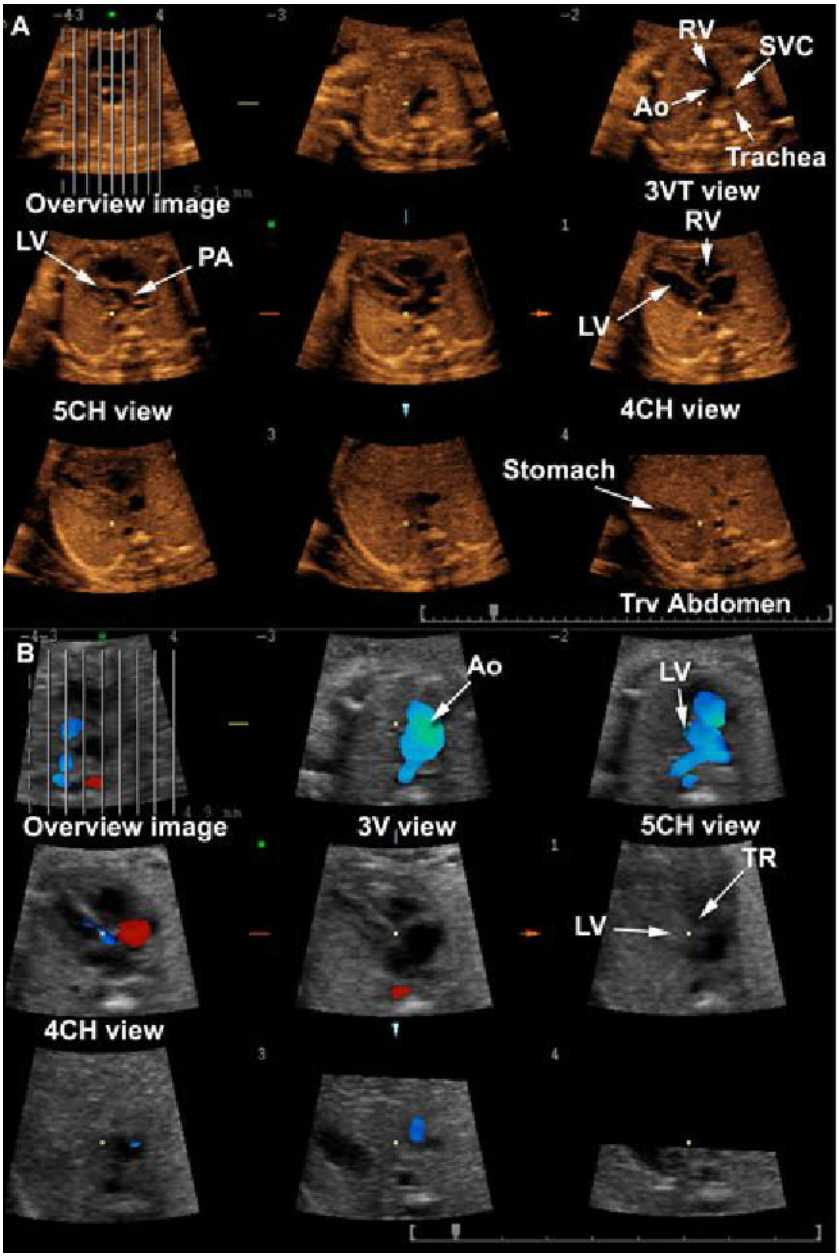

Figure 6.

Tomographic Ultrasound Imaging in a fetus with transposition of the great arteries. A) B-mode imaging. (1) In the three-vessel and trachea view, only the aorta is visualized, leaving the right ventricle; (2) the five chamber view demonstrates a vessel that bifurcates (pulmonary artery) connected to the left ventricle; (3) the four-chamber view is normal. B) Color Doppler imaging. (1) the three vessel view shows the aorta connecting to the right ventricle; (2) the pulmonary artery leaves the left ventricle and bifurcates. Legends: PA = pulmonary artery; Ao = aorta; RV = right ventricle; LV = left ventricle; 3V = three vessel; 3VT = three-vessel and trachea; SVC = superior vena cava; 4CH = four-chamber; 5CH = five-chamber; Trv = transverse

Table 1

American Institute of Ultrasound in Medicine guidelines for the examination of the four-chamber view.

General	Four cardiac chambers are present
	Majority of heart located in left chest
	Heart occupies about one-third of the thoracic area
	Normal cardiac situs, axis, and position
	Pericardial effusion not seen
Atria	Atria appear approximately equal in size
	Foramen ovale flap lies in the left atrium
	Lower rim of atrial septum (septum primum) is present
Ventricles	Ventricles approximately equal in size
	Ventricular septum appears intact from apex to crux
AV Valves	Both atrioventricular valves open and move freely
	Tricuspid valve septal insertion more apical than mitral valve

Reprinted with permission from the American Institute of Ultrasound in Medicine (AIUM) (Lee, JUM, 1998)

Table 2

Visualization rates for fetal heart structures displayed with TUI. All volume datasets acquired using STIC with B-mode imaging (n=195)

Cardiac view	Structures	Normal		Abnormal		Not diagnostic		Not present in the volume dataset	
		n	%	n	%	n	%	n	%
Upper abdomen		**123**	**63.1**	**2**	**1.0**	**70**	**35.9**		
	Stomach on the left side	129	66.2	2	1.0	-	-	64	32.8
	Aorta on the left side of spine	159	81.5	1	0.5	1	0.5	34	17.4
	IVC on the right side of spine	152	77.9	2	1.0	1	0.5	40	20.5
4CH view		**166**	**85.1**	**24**	**12.3**	**5**	**2.6**	**-**	**-**
	Four cardiac chambers present	188	96.4	3	1.5	4	2.1	3	1.5
	Majority of heart located in left chest	185	94.9	2	1.0	-	-	8	4.1
	Heart occupies about one-third of the thoracic area	185	94.9	-	-	-	-	10	5.1
	Normal cardiac situs, axis, and position	183	93.8	4	2.1	-	-	8	4.1
	Pericardial effusion not seen	192	98.5	1	0.5	2	1.0	-	-
	Atria appear approximately equal in size	183	93.8	4	2.1	8	4.1	-	-
	Foramen ovale flap lies in the left atrium	179	91.8	4	2.1	12	6.2	-	-
	Lower rim of atrial septum (septum primum) is present	183	93.8	4	2.1	8	4.1	-	-
	Ventricles approximately equal in size	183	93.8	9	4.6	3	1.5	-	-
	Ventricular septum appears intact from apex to crux	157	80.5	30	15.4	8	4.1	-	-
	Both atrioventricular valves open and move freely	185	94.9	4	2.1	6	3.1	-	-
	Tricuspid valve septal insertion more apical than mitral valve	177	90.8	6	3.1	4	2.1	-	-
5CH view		**154**	**79.0**	**18**	**9.2**	**24**	**12.3**		
	Aortic root emerging from the left ventricle	161	82.6	13	6.7	21	10.8	-	-
	IVS in continuity with the anterior wall of the ascending aorta	153	78.5	18	9.2	24	12.3	-	-
PA view		**93**	**47.7**	**8**	**4.1**	**2**	**1.0**	**92**	**47.2**
	PA visualized leaving the right ventricle	94	48.2	8	4.1	2	1.0	91	46.7
	At least one of the branches of PA bifurcating at its distal end	93	47.7	7	3.6	2	1.0	93	47.7
3VTV		**142**	**72.8**	**13**	**6.7**	**2**	**1.0**	**38**	**19.5**
	PA communicates directly with ductus arteriosus	145	74.4	8	4.1	3	1.5	39	20
	Transverse aortic arch between PA and SVC	154	79.0	8	4.1	4	2.1	29	14.9
	SVC visualized on the right side of the chest	161	82.6	3	1.5	2	1	29	14.9
	Trachea visualized posterior to SVC	146	74.9	1	0.5	6	3.1	42	21.5

Legends: 4CH: four-chamber; 5CH: five-chamber; 3VTV: three-vessel and trachea view; IVS: interventricular septum; SVC: superior vena cava; PA: pulmonary artery; STIC: spatiotemporal image correlation; IVC: inferior vena cava; TUI: Tomographic Ultrasound Imaging.

Table 3

Visualization rates for fetal heart structures displayed with TUI. All volume datasets were acquired with STIC and color Doppler imaging (n=168)

Cardiac view	Structures	Normal		Abnormal		Not diagnostic		Not present in the volume dataset	
		n	%	n	%	n	%	n	%
4CH view		**132**	**66.7**	**33**	**16.9**	**3**	**1.5**		
	Diastolic perfusion across the atrioventricular valves documented with color Doppler, with no evidence of valve regurgitation	152	77.9	14	7.2	2	1.0	-	-
	No color flow observed crossing the ventricular septum.	134	68.7	31	15.9	3	1.5	-	-
5CH view		**150**	**76.9**	**13**	**6.7**	**5**	**2.6**		
	Aortic root emerging from the left ventricle and the interventricular septum in continuity with the anterior wall of the ascending aorta	150	76.9	13	6.7	5	2.6	-	-
3VV		**134**	**68.7**	**11**	**5.6**	**23**	**11.8**		
	Aorta and pulmonary trunk converging toward the left thorax with the trachea to the right	138	70.8	9	4.6	-	-	21	10.8
	Pulmonary trunk with a slightly greater caliber than the aorta (ratio 1.2:1)	137	70.3	9	4.6	-	-	22	11.3
	Straight course of the vessels	139	71.3	9	4.6	-	-	20	10.3
	Antegrade flow through both great vessels throughout the cardiac cycle	137	70.3	9	4.6	-	-	22	11.3

Legends: 4CH: four-chamber; 5CH: five-chamber; 3VV: three-vessel view; TUI: Tomographic Ultrasound Imaging; STIC: spatiotemporal image correlation.

Table 4

Comparison of diagnostic information in TUI volume datasets acquired with B-mode imaging only or B-mode plus color Doppler imaging (n=168)

Plane of section	Perfect agreement between B-mode and color Doppler imaging in classifying views as normal, abnormal, or not diagnostic	Color Doppler modified the initial diagnostic impression by B-mode imaging only	No contribution of color Doppler to B-mode imaging	Kappa	P value by McNemar test
Four-chamber view	85.7% (145/168)	12.5% (21/168)*	1.8% (3/168)	0.537	0.135
Five-chamber view	83.9% (141/168)	14.2% (24/168)†	1.8% (3/168)	0.431	0.004
Three-vessel view	75% (126/168)	10.1% (17/168)‡	14.8% (25/168)	0.370	0.172

*In 3 cases, non-diagnostic four-chamber views were adequately visualized with color Doppler; 4 false-positive and 14 false-negative diagnoses by B-mode imaging were corrected by color Doppler.

†In 17 cases, a five-chamber view considered to be of no diagnostic value was adequately imaged by color Doppler; 6 false-positive and 1 false-negative diagnoses by B-mode imaging were corrected by color Doppler.

‡In 13 cases, a three-vessel view considered to be of no diagnostic value was adequately imaged by color Doppler; 1 false-positive and 3 false-negative diagnoses by B-mode imaging were corrected by color Doppler.

TUI: Tomographic Ultrasound Imaging.

J Perinat Med. Author manuscript; available in PMC 2006 March 1.

Table 5

Comparison of B-mode and color Doppler imaging in cardiac anomalies suspected by TUI, excluding isolated VSDs (n=16*)

Case #	GA	B-Mode Findings	View	B-Mode Diagnosis	Color Doppler Findings	View	Color Doppler Diagnosis
		Abnormal axis	4CH				
		VSD	4CH		VSD	4CH	
1	**23w5d**	Overriding Ao	5CH	**Tetralogy of Fallot**	Overriding Ao	5CH	**Tetralogy of Fallot**
		Narrow PA	3VTV		Color flow only in transverse aortic arch	3VV	
		Abnormal axis	4CH				
		ASD	4CH		ASD	4CH	
2	**29w4d**	VSD	4CH	**DORV, TGA, ASD, VSD**	VSD	4CH	**DORV, TGA, ASD, VSD**
		Hypoplastic RV	4CH		Hypoplastic RV	4CH	
		Ao leaves RV transposed	5CH		Ao leaves RV transposed	5CH	
		VSD	4CH				
3	**24w1d**	Overriding Ao	5CH	**Tetralogy of Fallot**	poor imaging, not diagnostic		—
		PA not visualized	3VTV				
4	**25w2d**	Transverse sections of Ao and azygous vein side by side	4CH	**Interrupted IVC with azygous continuation**	Transverse sections of aorta and azygous vein side by side	4CH	**Interrupted IVC with azygous continuation**
5	**32w1d**	Hypoplastic RV	4CH	**Hypoplastic RV**	Hypoplastic RV	4CH	**Hypoplastic RV, pulmonary atresia**
					PA not visualized	3VV	
		RV/LV disproportion	4CH		RV/LV disproportion	4CH	
6	**25w3d**	Narrow transverse aortic arch	3VTV	**Coarctation of the Aorta**	Narrow transverse aortic arch	3VTV	**Coarctation of the Ao, VSD**
					VSD	4CH	
		Dextrocardia	Abdom				
		Hypoplastic LV	4CH		Hypoplastic LV	4CH	
7	**19w3D**	VSD	4CH	**HLHS, DORV, TGA**			**HLHS, DORV, TGA**
		DORV	3VTV		DORV	3VV	
		TGA	5CH		TGA	5CH	
		RV/LV disproportion	4CH		RV/LV disproportion	4CH	
8	**36w4d**			**RV/LV disproportion**	Narrow transverse aortic arch	3VV	**Coarctation of the Ao**
					Reverse flow transverse aortic arch	3VV	
		ASD	4CH		ASD	4CH	
9	**16w6d**	VSD	4CH	**AV canal**	VSD	4CH	**AV canal**
		Single AV valve	4CH		Single AV valve	4CH	
11	**31w3d**			**HLHS**	Hypoplastic LV	4CH	**HLHS**
		Hypoplastic LV	4CH		Tricuspid regurgitation	4CH	
		Ao not visualized leaving LV	5CH		Ao not visualized leaving LV	5CH	
		Ao not visualized in 3VTV	3VTV		Ao not visualized in 3VTV	3VTV	
		VSD	4CH		VSD	4CH	
12	**22w6d**	Overriding Ao	5CH	**Tetralogy of Fallot**	Overriding Ao	5CH	**Tetralogy of Fallot**
		PA not visualized	3VTV		PA smaller than Ao	3VV	
		Abnormal axis	4CH				
13	**20w3d**	Ao leaving RV	3VTV	**TGA**	Ao leaving RV	3VTV	**TGA**
		PA leaving LV	5CH		PA leaving LV	5CH	
14	**22w3d**	Poor imaging, not diagnostic		—	Transverse sections of Ao and azygous vein side by side	4CH	**Interrupted IVC with azygous continuation**
		Hypoplastic RV	4CH		Hypoplastic RV	4CH	
15	**29w4d**			**Pulmonary atresia**	Tricuspid regurgitation	4CH	**Pulmonary atresia**

Case #	GA	B-Mode Findings	View	B-Mode Diagnosis	Color Doppler Findings	View	Color Doppler Diagnosis
		Absent PA	3VTV		Retrograde perfusion of PA	3VV	
		Ao leaving RV	3VTV		Ao leaving RV	3VTV	
16	**28w0d**	PA leaving LV	5CH	**TGA**	PA leaving LV	5CH	**TGA**
		VSD	4CH		VSD	4CH	
17	**19w3d**	Parallel arteries leaving LV and RV	5CH	**TGA**	Overriding Ao	5CH	**Tetralogy of Fallot**
					PA not visualized	3VTV	

Legend: DORV: double outlet right ventricle; TGA: transposition of the great arteries; ASD: atrial septal defect; VSD: ventricular septal defect; IVC: inferior vena cava; RV: right ventricle; LV: left ventricle; HLHS: hypoplastic left heart syndrome; AV: atrioventricular; PA: pulmonary artery; Ao: aorta; 3VTV: three-vessel and treachea view; 3VV: three-vessel view; 4CH: four-chamber; 5CH: five-chamber; TUI: Tomographic Ultrasound Imaging.

*Case 10 (displayed in Table 6) was a rhabdomioma that was not visualized by TUI, either with B-mode or color Doppler imaging.

Table 6

Comparison of prenatal diagnosis by TUI (B-mode imaging and color Doppler and postnatal diagnosis (n=17).

Case #	GA	TUI Diagnosis	Postnatal Diagnosis
1	23w5d	Tetralogy of Fallot	Tetralogy of Fallot
2	29w4d	DORV, TGA, ASD, VSD	DORV, TGA, ASD, VSD
3	24w1d	Tetralogy of Fallot	TGA
4	25w2d	Interrupted IVC with azygous continuation	Interrupted IVC with azygous continuation
5	25w3d	Coarctation of the aorta, VSD	Coarctation of the aorta, VSD
6	19w3d	HLHS, DORV, TGA	HLHS, DORV, TGA*
7	36w4d	Coarctation of the aorta	Normal
8	16w6d	AV canal	AV canal
9	31w3d	HLHS	HLHS
10	20w6d	Normal	Rhabdomioma
11	22w6d	Tetralogy of Fallot	Lost to follow-up
12	20w3D	TGA	TGA
13	22w3d	Interrupted IVC with azygous continuation	Interrupted IVC with azygous continuation
14	37w0d	Severe tricuspid regurgitation	Ebstein anomaly
15	29w4d	Pulmonary atresia	Pulmonary atresia
16	28w0d	TGA	TGA
17	19w3d	Tetralogy of Fallot	Lost to follow-up

Legend: DORV: double outlet right ventricle; TGA: transposition of the great arteries; ASD: atrial septal defect; VSD: ventricular septal defect; IVC: inferior vena cava; RV: right ventricle; LV: left ventricle; HLHS: hypoplastic left heart syndrome; AV: atrioventricular; TUI: Tomographic Ultrasound Imaging.

* In case #7, the diagnosis was confirmed in the prenatal period independently by a pediatric cardiologist. The pregnancy was lost to follow-up and no neonatal information was available.

Table 7

Sensitivity, specificity, positive- and negative-predictive values of TUI to detect congenital heart disease.

	# of patients available for analysis	Prevalence	Sensitivity	Specificity	Positive predictive value	Negative predictive value
B-mode imaging	115[†]	12.2% (14/115)	85.7% (12/14)	100.0% (101/101)	100.0% (12/12)	98.0% (101/103)
Color Doppler	98[‡]	14.3% (14/98)	92.9% (13/14)	98.8% (83/84)	92.9% (13/14)	98.8% (83/84)

[†]Complete follow-up was available in 131/172 patients scanned by B-mode imaging (76.2%) (excluding cases of isolated VSDs). Sixteen patients were excluded from this portion of the analysis: one patient whose images were interpreted as tetralogy of Fallot but who was found at the time of surgery to have a subaortic VSD associated with transposition of the great arteries, and 15 patients whose ultrasonographic images were considered to be of poor diagnostic quality.

[‡]Complete follow-up was available in 105/142 patients scanned by color Doppler (61.0%) (excluding cases of isolated VSDs). Seven patients were excluded from this portion of the analysis: in all cases, the ultrasonographic images were considered to be of poor diagnostic quality.

TUI: Tomographic Ultrasound Imaging; VSF: ventricular septal defects.